

See discussions, stats, and author profiles for this publication at: <https://www.researchgate.net/publication/49648929>

# 1,3-Diamido-calix[4]arene Conjugates of Amino Acids: Recognition of -COOH Side Chain Present in Amino Acids, Peptides, and Proteins by Experimental and Computational Studies

ARTICLE *in* THE JOURNAL OF ORGANIC CHEMISTRY · JANUARY 2011

Impact Factor: 4.72 · DOI: 10.1021/jo101759f · Source: PubMed

---

CITATIONS

25

READS

34

## 4 AUTHORS, INCLUDING:



Balaji Ramanujam

Central University of Tamil Nadu

16 PUBLICATIONS 348 CITATIONS

[SEE PROFILE](#)



Jugun prakash Chinta

Hebrew University of Jerusalem

17 PUBLICATIONS 220 CITATIONS

[SEE PROFILE](#)

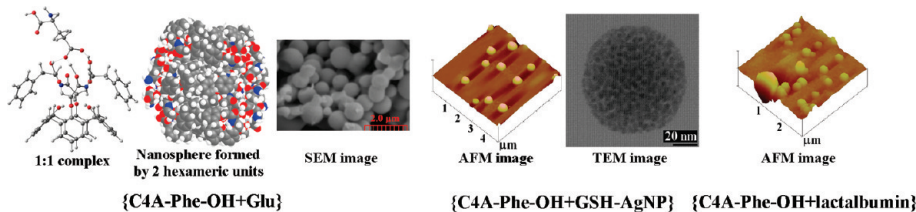
# 1,3-Diamido-calix[4]arene Conjugates of Amino Acids: Recognition of –COOH Side Chain Present in Amino Acids, Peptides, and Proteins by Experimental and Computational Studies

Amitabha Acharya, Balaji Ramanujam, Jugun Prakash Chinta, and Chebrolu P. Rao\*

*Bioinorganic Lab, Department of Chemistry, Indian Institute of Technology Bombay, Powai, Mumbai 400 076, India*

cprao@iitb.ac.in

Received September 10, 2010



Lower rim 1,3-diamido conjugates of calix[4]arene have been synthesized and characterized, and the structures of some of these have been established by single crystal XRD. The amido-calix conjugates possessing a terminal –COOH moiety have been shown to exhibit recognition toward guest molecules possessing –COOH moiety, viz., Asp, Glu, and reduced and oxidized glutathione (GSH, GSSG), by switch-on fluorescence in aqueous acetonitrile and methanol solutions when compared to the control molecules via forming a 1:1 complex. The complex formed has been shown by mass spectrometry, and the structural features of the complexes were derived on the basis of DFT computations. The association constants observed for the recognition of Asp/Glu by Phe-calix conjugate, viz.,  $532/676 \text{ M}^{-1}$ , are higher than that reported for the recognition of Val, Leu, Phe, His, and Trp ( $16-63 \text{ M}^{-1}$ ) by a water-soluble calixarene (Arena, G., et al. *Tetrahedron Lett.* **1999**, *40*, 1597). For this recognition, there should be a free –COOH moiety from the guest molecule. AFM, SEM, and DLS data exhibited spherical particles with a hundred-fold reduction in the size of the complexes when compared to the particles of the precursors. These spherical particles have been computationally modeled to possess hexameric species reminiscent of the hexameric micellar structures shown for a  $\text{Ag}^+$  complex of a calix[6]arene reported in the literature (Houmadi, S., et al. *Langmuir* **2007**, *23*, 4849). Both AFM and TEM studies demonstrated the formation of nanospheres in the case of GSH-capped Ag nanoparticles in interaction with the amido-calix conjugate that possesses terminal –COOH moiety. The AFM studies demonstrated in this paper have been very well applied to albumin proteins to differentiate the aggregational behavior and nanostructural features exhibited by the complexes of proteins from those of the uncomplexed ones. To our knowledge, this is the first report wherein a amido-calix[4]arene conjugate and its amino acid/peptide/protein complexes have been differentiated on the basis of spectroscopy and microscopy studies followed by species modeling by computations.

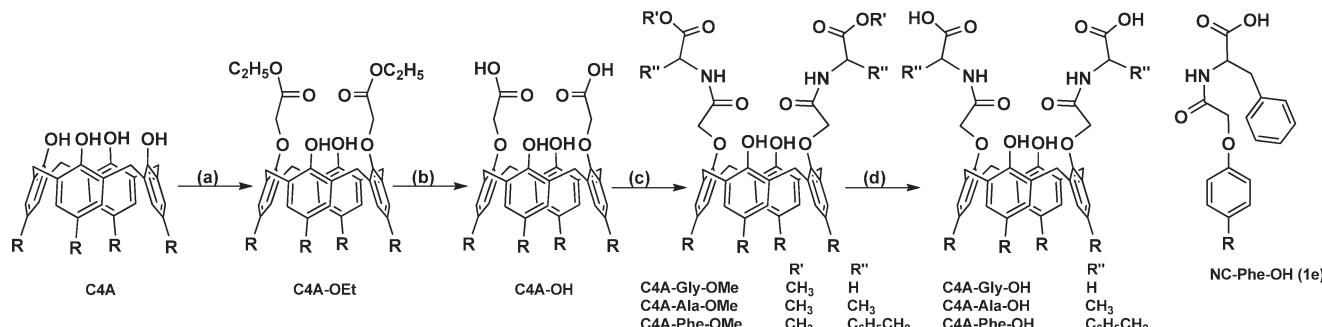
## Introduction

Amino acids possessing side chain –COOH functionality, viz., aspartic acid and glutamic acid, and peptides, GSH (reduced glutathione) GSSG (oxidized glutathione), and

proteins containing these are of prime interest in biological systems.<sup>1–3</sup> Asp and Glu are known to play important roles as excitatory amino acid neurotransmitters in the central nervous system of mammals, whereas GSH is known to protect intracellular components against oxidative damage

(1) Marc, R. E.; Lam, D. M. *Proc. Natl Acad. Sci. U.S.A.* **1981**, *78*, 7185.  
(2) Mizrahi, V.; Brooksbank, R. L.; Nkabinde, N. C. *J. Biol. Chem.* **1994**, *269*, 19245.

(3) Voet, D.; Voet, J. G. *Biochemistry*; John Wiley & Sons: New York, 1990.

SCHEME 1. Synthesis of the Precursors and Amido-calix Conjugates<sup>a</sup>

<sup>a</sup> Reagents and conditions: (a) acetone,  $K_2CO_3$ ,  $BrCH_2COOEt$ , reflux for 15 h; (b) EtOH, aq NaOH, reflux for 24 h; (c) HCl salt of the ester of the corresponding amino acid, dry THF,  $Et_3N$ , HOBT, DCC; (d) THF, LiOH. Similar method has been used for the synthesis of NC-Phe-OH (1e), where *p*-*tert*-butyl phenol has been used instead of C4A (Supporting Information). R = *tert*-butyl. Compounds 1a–1d are given in Scheme 3.

and also in detoxifying heavy metal ions by using its mercapto groups.<sup>4</sup> Concentration changes of Asp and Glu levels in certain regions of the brain are closely related to Parkinson's disease.<sup>5–7</sup> Therefore, the recognition of such amino acids, peptides, and proteins possessing –COOH moieties is a challenging task. Molecular systems capable of recognizing these by eliciting easily detectable spectroscopic signals and microscopic structures are of paramount importance. Recently, a galactosyl based naphthalyl-imine derivative has been shown to recognize Glu by fluorescence spectroscopy.<sup>8</sup> A set of organic and inorganic molecular species have been employed in combination as receptor units for the identification of naturally occurring amino acids by indicator displacement assays controlled by pH.<sup>9</sup> Calix[4]arene provides a congenial platform for bringing appropriate functionalization and hence acts as useful molecular framework. Such systems are expected to yield interesting nanostructural features in interaction with the guest species. Water-soluble calixarenes have also been shown to complex Val, Leu, Phe, His, and Trp with  $K_a$  values in the range of 16–63 M<sup>-1</sup>.<sup>10</sup> Sulfonato-calix[6]arene has been shown to complex basic amino acids, viz., Lys and Arg, and their peptides as studied by <sup>1</sup>H NMR and microcalorimetry.<sup>11–13</sup> Some were shown to exhibit enantioselective differentiation<sup>14,15</sup> as well as amino acid transport.<sup>16</sup> Thus, the importance of calix[4]arene conjugates as biosensors for amino acids and peptides has been

noted in the literature, though the examples of such systems were limited.<sup>10–12,16–21</sup> Recently our group reported the selective recognition of amino acids by the metal ion complexes of calix[4]arene conjugates.<sup>22–24</sup>

To our knowledge, none of the calixarene derivative have been reported for the detection of Asp, Glu, or GSH. Therefore, the present paper demonstrates for the first time the selective recognition of Asp, Glu, and GSH by lower rim 1,3-diamido conjugates of calix[4]arene possessing terminal –COOH moieties by fluorescence spectroscopy wherein the complex species formed have been further studied by DFT calculations. The nanoscopic aggregate formation of these amido-calix[4]arene conjugates with Asp or Glu has been shown by scanning electron microscopy (SEM) and atomic force microscopy (AFM), and the nanospheres formed with the GSH-coated Ag nanoparticles by transmission electron microscopy (TEM) as well as by AFM. The utility of the amido-calix conjugates has been further extended even to proteins to show their novel nanostructural features by microscopy.

## Results and Discussion

The amido-calix[4]arene conjugates have been synthesized in four steps starting from simple *p*-*tert*-butyl-calix[4]-arene (C4A) as given in Scheme 1.<sup>25</sup> All synthetic compounds (Scheme 1) were checked for their purity and authenticity and were characterized by NMR, FTIR, and ESI MS as given in the Experimental Section.<sup>26</sup> Since the terminals of

- (4) Mehra, R. K.; Tran, K.; Scott, G. W.; Mulchandani, P.; Saini, S. S. *J. Inorg. Biochem.* **1996**, *61*, 125.
- (5) Xin, L.; Jie, L.; Liu, C.-W.; Zhao, S.-L. *Chin. J. Anal. Chem.* **2007**, *35*, 1151.
- (6) Sonsalla, P. K.; Nicklas, W. J.; Heikkila, R. E. *Science* **1989**, *243*, 398.
- (7) Fornai, F.; Vaglini, F.; Maggio, R.; Bonuccelli, U.; Corsini, G. U. *Neurosci. Biobehav. Rev.* **1997**, *21*, 401.
- (8) Ahuja, R.; Singh, N. K.; Ramanujam, B.; Ravikumar, M.; Rao, C. P. *J. Org. Chem.* **2007**, *72*, 3430.
- (9) Buryak, A.; Severin, K. A. *J. Am. Chem. Soc.* **2005**, *127*, 3700.
- (10) Arena, G.; Contino, A.; Gulino, F. G.; Magri, A.; Sansone, F.; Sciotto, D.; Ungaro, R. *Tetrahedron Lett.* **1999**, *40*, 1597.
- (11) Douteau-Guevel, N.; Coleman, A. W.; Morel, J.-P.; Morel-Desrosiers, N. *J. Chem. Soc., Perkin Trans. 2* **1999**, *3*, 629.
- (12) Douteau-Guevel, N.; Coleman, A. W.; Morel, J.-P.; Morel-Desrosiers, N. *J. Phys. Org. Chem.* **1998**, *11*, 693.
- (13) Douteau-Guevel, N.; Perret, F.; Coleman, A. W.; Morel, J.-P.; Morel-Desrosiers, N. *J. Chem. Soc., Perkin Trans. 2* **2002**, *3*, 524.
- (14) Liu, S.; He, Y.; Qing, G.; Xu, K.; Qin, H. *Tetrahedron: Asymmetry* **2005**, *16*, 1527.
- (15) Liu, F.; Lu, G.-Y.; He, W.-J.; Liu, M.-H.; Zhu, L.-G. *Thin Solid Films* **2004**, *468*, 244.
- (16) Antipin, I. S.; Stoikov, I. I.; Pinkhassik, E. M.; Fitseva, N. A.; Stibor, I.; Konovalov, A. I. *Tetrahedron Lett.* **1997**, *38*, 5865.

- (17) Selkti, M.; Tomas, A.; Coleman, A. W.; Douteau-Guevel, N.; Nicolis, I.; Villain, F.; de Rango, C. *Chem. Commun.* **2000**, *2*, 161.
- (18) Buschmann, H.-J.; Mutthac, L.; Jansen, K. *J. Inclusion Phenom. Macrocyclic Chem.* **2001**, *39*, 1.
- (19) Hassen, W. M.; Martelet, C.; Davis, F.; Higson, S. P. J.; Abdelghani, A.; Helali, S.; Jaffrezic-Renault, N. *Sens. Actuators, B* **2007**, *124*, 38.
- (20) Lu, J. Q.; Zhang, L.; Sun, T. Q.; Wang, G. X.; Wu, L. Y. *Chin. Chem. Lett.* **2006**, *17*, 575.
- (21) Lazar, A. N.; Danylyuk, O.; Suwinska, K.; Coleman, A. W. *J. Mol. Struct.* **2006**, *825*, 20.
- (22) Joseph, R.; Ramanujam, B.; Acharya, A.; Rao, C. P. *J. Org. Chem.* **2009**, *74*, 8181.
- (23) Jugun, P. C.; Acharya, A.; Kumar, A.; Rao, C. P. *J. Phys. Chem. B* **2009**, *113*, 12075.
- (24) Joseph, R.; Jugun, P. C.; Rao, C. P. *J. Org. Chem.* **2010**, *75*, 3387.
- (25) Collins, E. M.; McKervey, M. A.; Madigan, E.; Moran, M. B.; Owens, M.; Ferguson, G.; Harris, S. J. *J. Chem. Soc., Perkin Trans. I* **1991**, *12*, 3137.
- (26) Gutsche, C. D.; Dhawan, B.; No, K. H.; Muthukrishnan, R. *J. Am. Chem. Soc.* **1981**, *103*, 3782.

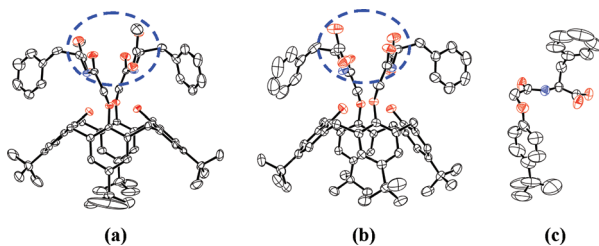


**FIGURE 1.** ORTEP diagrams of the molecular structures of (a) C4A-Phe-OMe, (b) C4A-Phe-OH, and (c) NC-Phe-OH as determined by single crystal XRD. Encircled portion possesses sites for interaction.

**TABLE 1. Crystallographic Parameters for the Structure Determination and Refinement**

	C4A-Phe-OMe	NC-Phe-OH
empirical formula	2(C <sub>68</sub> H <sub>82</sub> N <sub>2</sub> O <sub>10</sub> ) H <sub>2</sub> O	C <sub>21</sub> H <sub>25</sub> NO <sub>4</sub>
temperature (K)	120	150
crystal system	monoclinic	orthorhombic
space group	P2 <sub>1</sub> (No. 4)	P2 <sub>1</sub> 2 <sub>1</sub> 2 <sub>1</sub> (No. 19)
a/Å	14.4663(4)	7.594(3)
b/Å	26.1325(7)	9.670(3)
c/Å	17.0631(5)	27.818(8)
β/deg	96.133(3)	
volume/Å <sup>3</sup>	6413.6(3)	2042.8(12)
Z	2	4
reflections collected	66808	16584
independent reflections	22341	3593
R <sub>int</sub>	0.103	0.092
reflections used [I > 2.0σ(I)]	13689	1328
parameters	1478	250
final R	0.0863	0.0448
R' <sub>w</sub> <sup>a</sup>	0.1814	0.1033

<sup>a</sup>w = 1/[s<sup>2</sup>(F<sub>o</sub><sup>2</sup>) + (0.0553P)<sup>2</sup> + 4.9051P] in the case of C4A-Phe-OMe; w = 1/[s<sup>2</sup>(F<sub>o</sub><sup>2</sup>) + (0.0440P)<sup>2</sup>] in the case of NC-Phe-OH; where P = (F<sub>o</sub><sup>2</sup> + 2F<sub>c</sub><sup>2</sup>)/3.

both pendants of these conjugates possess a —COOH moiety, it is of interest to study their recognition abilities toward biologically important molecules, such as amino acids and peptides. To elicit the selectivity of these conjugates (C4A-Phe-OH, C4A-Gly-OH, and C4A-Ala-OH) as well as the role of the two amido arms, appropriate control molecular systems were generated by converting the —COOH terminal into —COOR {e.g., C4A-Phe-OMe, C4A-Gly-OMe, and C4A-Ala-OMe}, and a single strand version of these, namely, NC-Phe-OH, and a nonamido version of these, namely, {C4A-OEt, C4A-OH},<sup>27</sup> were synthesized and characterized (Schemes 1 and 3; Experimental Section) and were used in the titration studies (Supporting Information).

**Crystal Structures.** Single crystals of C4A-Phe-OMe and NC-Phe-OH were obtained by slow evaporation of their ethanol solutions. These crystals yielded satisfactory diffraction data suitable to determine their 3-D structures. (Figure 1a,c). The corresponding details of the structure determination and refinement are given in Table 1 (Supporting Information). The crystal structure of C4A-Phe-OMe exhibited cone conformation for the calix[4]arene and is in conformity with the results obtained on the basis of NMR. The structure exhibits rather exposed amide and ester moieties that are amenable for interaction with the incoming

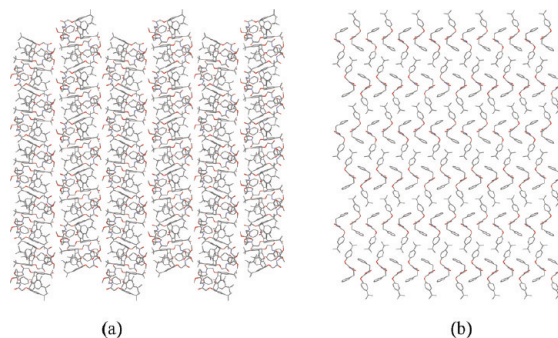


**FIGURE 2.** Lattice structures of (a) C4A-Phe-OMe and (b) NC-Phe-OH, as viewed down “c” and “a”, respectively.

species. Similar structural features were observed even with C4A-Phe-OH where the terminal —COOH is poised suitable for interaction (Figure 1b).<sup>28</sup> Comparison of the amido arm present in the structures of C4A-Phe-OMe and C4A-Phe-OH with that present in the noncalixarene conjugate, NC-Phe-OH, exhibits considerable changes in the dihedral angles (Supporting Information) of the arm, and hence the side chain phenyl moiety is more exposed. This difference is expected to reflect on their ability to interact with the incoming moiety. This has indeed been seen from the titrations carried out by fluorescence spectroscopy. In the crystal lattice, the C4A-Phe-OMe stacks in the form of columns wherein the adjacent pair is arranged in a head-to-tail fashion (Figure 2a). The water of crystallization indeed connects the amido-calix conjugates through hydrogen bond interactions and thus forms a supramolecular structure. However, the lattice of the single strand derivative, namely, NC-Phe-OH, does not show such supramolecular formation (Figure 2b).

**Necessity of the Amido-calix[4]arenes for the Selective Recognition of Asp, Glu, GSH, and GSSG.** All fluorescence spectral studies were carried out using 5 μM solutions of the amido-calix[4]arene conjugate. When C4A-Phe-OH is excited at 280 nm, it exhibits a strong emission around 313 nm. All titrations of C4A-Phe-OH with 20 naturally occurring amino acids revealed that only the Asp and Glu exhibits an increase in fluorescence intensity, while the others exhibit no significant change (Figure 3a,c). The enhancement is 3.5- to 4.0-fold in methanol (Supporting Information), and it is 5.5- to 6.0-fold in 1:1 aqueous acetonitrile (Supporting Information). The fluorescence intensity data fit well with a 1:1 complex formed between C4A-Phe-OH and Asp/Glu by exhibiting K<sub>a</sub> values of 532/676 M<sup>-1</sup>. These association constants are much higher than that observed for Val, Leu, Phe, His, and Trp (16–63 M<sup>-1</sup>) in the literature in the case of a water-soluble calix[4]arene.<sup>10</sup> Titration of C4A-Phe-OH with the totally esterified Asp/Glu, viz., Asp-(OBz)<sub>2</sub> or Glu-(OMe)<sub>2</sub>, exhibited no change in the fluorescence intensity during the titration (Supporting Information). Combining this result with that observed in the case of other naturally occurring amino acids suggests the involvement of the side chain carboxylic group in the interaction and not the C<sup>α</sup> bound groups. Thus Asp and Glu elicit fluorescence response by switch-on mechanism, and hence only these two amino acids are amenable for sensing by C4A-Phe-OH,

(27) Joseph, R.; Ramanujam, B.; Acharya, A.; Khutia, A.; Rao, C. P. *J. Org. Chem.* **2008**, 73, 5745.

(28) Dey, M.; Rao, C. P. Unpublished results.

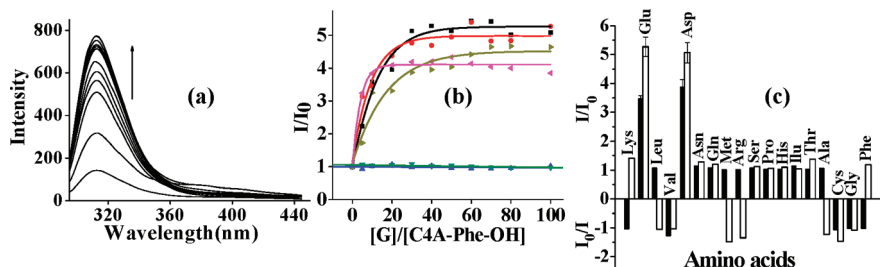


**FIGURE 3.** Fluorescence titration of C4A-Phe-OH with amino acids: (a) spectral traces obtained in the titration with Asp in 1:1 H<sub>2</sub>O/CH<sub>3</sub>CN; (b) plots of relative fluorescence intensity ( $I/I_0$ ) of the titrations of Asp (black ■), Glu (red ●), Asp ester (blue ▲), Glu ester (green ▼), GSH (pink left-facing triangle), and GSSG (gray right-facing triangle) (G = guest species); (c) histogram showing the number of times of enhancement (positive axis) or quenching (negative axis) of fluorescence intensity of C4A-Phe-OH when titrated with amino acids. Filled bars are for methanol (at 200 equiv), and unfilled ones are for aqueous acetonitrile (at 100 equiv) solutions. Error bars are given based on three different measurements.

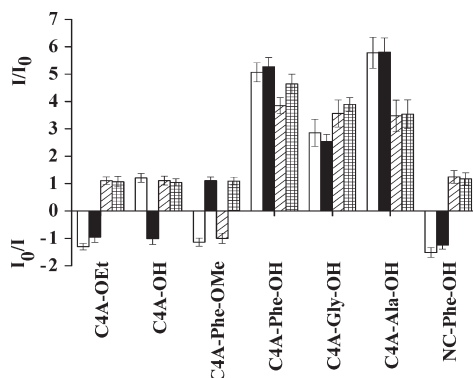


**FIGURE 4.** Histogram showing the number of times of enhancement (positive axis) or quenching (negative axis) of fluorescence intensity in the titration of amido-calix conjugates and other control molecules with Asp (open bar), Glu (black bar), GSH (lined bar), and GSSG (cross-hatched bar) in aqueous acetonitrile (at 100 equiv). Similar results have also been obtained in methanol (Supporting Information).

among the 20 naturally occurring amino acids. Similar results were observed when a tripeptide, namely, GSH, possessing  $\gamma$ -glutamyl moiety or its oxidized form, namely, GSSG, was used in the titration (Figure 3b). This further supports the involvement of  $-COOH$  moiety in the recognition, besides ruling out the involvement of the  $-SH$  moiety. The latter has indeed been supported by the titrations carried out with Cys. Thus C4A-Phe-OH has been clearly shown to be selective toward Asp and Glu among the 20 amino acids studied in addition to the tripeptides, GSH and GSSG.

**Involvement of the Amido Arms in the Recognition.** Comparison of the fluorescence titration results of the C4A-OH and C4A-OEt with those of the amido conjugates clearly suggests the necessity of the amido arm in the recognition process. On the other hand, the comparison of the fluorescence titration results of NC-Phe-OH with that of the C4A-Phe-OH supports the necessity of the calix[4]arene platform in the recognition process (Supporting Information) (Figure 4).

**Involvement of the Side Chain Moiety in the Recognition.** To see the involvement of the side chain of the amido arm of the conjugate in the recognition process, similar fluorescence titrations were carried out using C4A-Gly-OH and C4A-Ala-OH. The corresponding data was compared with that of

the C4A-Phe-OH (Figure 4), and it was found that there is no role of side chain in the recognition process.

**Involvement of the Terminal  $-COOH$  Moiety on the Amido Arms in the Recognition.** The esters of these, namely, C4A-Gly-OMe and C4A-Ala-OMe, do not show any change in the fluorescence, suggesting the necessity of the terminal  $-COOH$  moiety on the arm (Supporting Information) (Figure 4).

All of the fluorescence titration results together clearly suggest that the calix[4]arene platform, the amido arm as well as the terminal  $-COOH$  group of the host, and the side chain  $-COOH$  of the guest species are essential for the recognition. Thus the amido-calix conjugates selectively recognize Asp, Glu, GSH, and GSSG.

**ESI MS Studies.** The stoichiometry of the complexes formed between Glu/GSH and amido-calix[4]arene conjugates has been established to be 1:1 by the molecular ion peaks observed in ESI MS spectrometry (Supporting Information). These are found at 1206.7/1366, 1026.5/1186.6, and 1054.6/1214.7, respectively, for the amido conjugates, namely, C4A-Phe-OH, C4A-Gly-OH, and C4A-Ala-OH, indicating the formation of their 1:1 complexes with Glu/GSH. To our knowledge, there is only one paper in the literature in which the complex formed between O-ethylated calix[6]arene and His/Lys or Arg has been shown by mass spectrometry.<sup>29</sup> The structural features of the complexes formed in the present case have been computed on the basis of DFT calculations.

**Computational Modeling of the Complex Formed between Amido-calix Conjugate and Asp, Glu, and GSH.** To address the structural features of the complexes formed between the amido-calix conjugates, C4A-Phe-OH'/C4A-Gly-OH' and Asp/Glu/GSH, computational modeling studies have been carried out by geometry optimizations using the Gaussian 03 package<sup>30</sup> as per the details given in the Experimental Section. The final structure of the optimized complex obtained through DFT calculations exhibits the presence of three hydrogen bonds between the side chain  $-COOH$  of Asp/Glu/GSH and the two arms of C4A-Phe-OH'/C4A-Gly-OH' (Figure 5a–c; Supporting Information). Such 1:1 complexation leads to a stabilization of  $-24$  to  $-27$  kcal/mol in the case of all the three complexes. This is comparable with that obtained

(29) Stone, M. M.; Franz, A. H.; Lebrilla, C. B. *J. Am. Soc. Mass Spectrom.* **2002**, *13*, 964.

(30) Frisch, M. J. et al. *Gaussian 03, Revision C.02*; Gaussian, Inc.: Wallingford, CT, 2004.

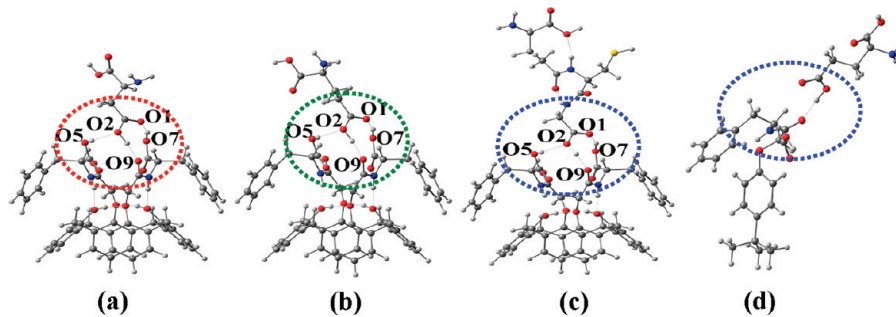


**FIGURE 5.** Structure of the DFT optimized amino acid complexes of C4A-Phe-OH' and NC-Phe-OH: (a) {C4A-Phe-OH' + Asp}, (b) {C4A-Phe-OH' + Glu}, (c) {C4A-Phe-OH' + GSH}, and (d) {NC-Phe-OH + Glu}. Encircled portions show the region of interaction. Visualization has been performed by using Chemcraft.<sup>32</sup>

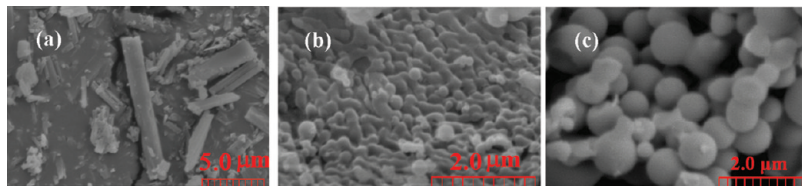


**FIGURE 6.** Scanning electron micrographs of (a) C4A-Phe-OH, (b) {C4A-Phe-OH + Asp}, and (c) {C4A-Phe-OH + Glu}.

from the literature (i.e.,  $-21$  to  $-28$  kcal/mol) by plugging in the H $\cdots$ A distances of the optimized structure (Supporting Information).<sup>31</sup> On the other hand, the computations carried out with the single strand version, viz., NC-Phe-OH showed only one hydrogen bond (Figure 5d).

**Spherical Clusters Formed between C4A-Phe-OH and Asp or Glu.** Because calixarene systems are known to exhibit supramolecular structures, it is of interest to see whether there are any changes in the microscopic architectural features of the amido conjugate and its complexes by microscopy studies.

**SEM Studies.** While the SEM micrographs of C4A-Phe-OH exhibit crystalline rods of  $(0.4\text{--}1.4) \times (2.8\text{--}11.1)\text{ }\mu\text{m}^2$  (Figure 6a), its complex {C4A-Phe-OH + Asp} exhibits almost uniformly distributed spherical surfaces with a size distribution of 200–300 nm (Figure 6b). Similar results were obtained even for the complex, {C4A-Phe-OH + Glu}, but the size of particles range from 400 to 600 nm (Figure 6c). The SEM features of C4A-Phe-OH and its complex {C4A-Phe-OH + Asp} are quite different from that of the simple Asp (Supporting Information). Thus the microscopic features of the amido conjugate differ substantially from its complexes.

**AFM Studies.** The shape and size of the particles observed in the AFM image of C4A-Phe-OH (Figure 7a) differ largely from that of its complex, {C4A-Phe-OH + Asp} (Figure 7b), suggesting that the complex can be easily differentiated from its precursor amido-calix conjugate. While C4A-Phe-OH exhibits uniformly distributed particles of 225–250 nm, its Asp complex exhibits marginally elongated spherical ones 75–110 nm in size that were also distributed uniformly. However, both exhibited clusters that were formed from basic units, where the ratio of the smaller to the cluster particles was found to be  $\sim 1:2$ . Height of these particles is much smaller in the complex (7–16 nm) as compared to the

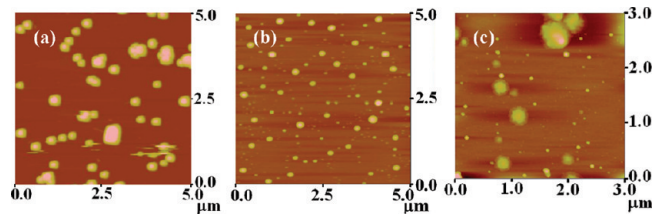


**FIGURE 7.** Atomic force microscopy images of (a) C4A-Phe-OH, (b) {C4A-Phe-OH + Asp}, and (c) {C4A-Phe-OH + Glu}.

same in the precursor amido conjugate (93–159 nm), indicating a drastic shrinking of the particle size in the complex and thereby bringing a volume reduction of  $\sim 100$ -fold. Thus the volume and shape of the particles differ drastically between the precursor conjugate and its Asp complex. Similar results have also been obtained for the Glu complex, {C4A-Phe-OH + Glu} (Figure 7c) (Supporting Information).

**Dynamic Light Scattering (DLS) Studies.** DLS experiments carried out with C4A-Phe-OH, {C4A-Phe-OH + Asp}, and {C4A-Phe-OH + Glu} exhibited average aggregates of 405, 66, and 110 nm, respectively, indicating a volume reduction of at least 100-fold in the aggregates upon complexation when compared to the uncomplexed C4A-Phe-OH.

Thus all three techniques, viz., AFM, SEM, and DLS, suggest a reduction in the surface area of the particles by about 100-fold upon complexation when compared to the particles of C4A-Phe-OH owing to the nature of the growth of the particles in each of this case. Thus, to our knowledge, this is the first calixarene conjugate that has been demonstrated to recognize amino acids and peptides based on microscopy studies.

**Computational Modeling of the Spherical Cluster.** The spherical clusters observed from microscopy for the Asp or Glu complex of C4A-Phe-OH may result from the aggregation of the originally formed 1:1 complexes already given in this paper. Because Glu exhibits dimers to hexamers in solution to an extent of  $>90\%$  of the species as established

(31) Grabowski, S. J. *Annu. Rep. Prog. Chem., Sect. C* 2006, 102, 131.

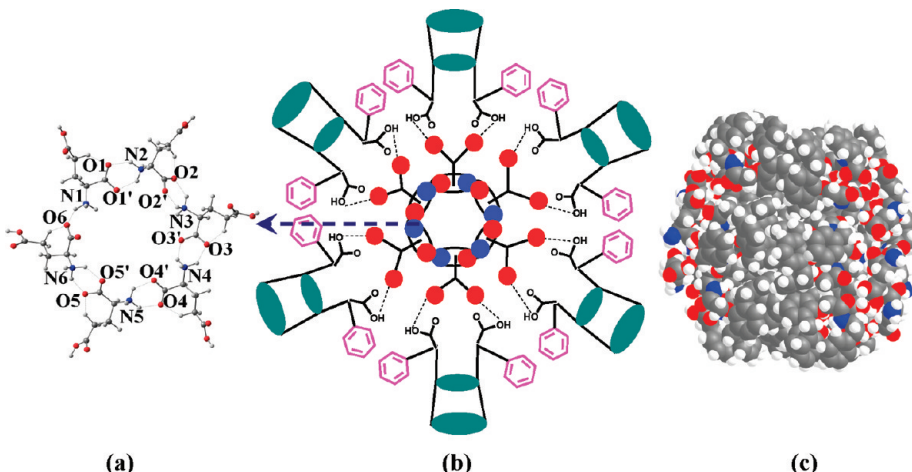


**FIGURE 8.** (a) A PM3 optimized hexamer of Glu. (b) Proposed model for the species formed from 1:1 Asp/Glu complexes of C4A-Phe-OH. Inner core represents the hexameric closed cluster formed by the Asp/Glu units. The amino end (blue) of one of the amino acids interacts with the carboxylic end (red) of the neighbor. The green cups represent calixarene units. (c) Space-filling model of the hexameric aggregate of {C4A-Phe-OH' + Glu} obtained from geometry minimization using HYPERCHEM program, shown as the dimer formed by two such aggregates.

by mass spectrometry,<sup>33</sup> it might be appropriate to start the modeling from one such species. The oligomers of Ser and Pro have been computationally modeled.<sup>34,35</sup> Therefore, in order to emerge with the spherical nature of the particles, a hexamer of simple Glu has been modeled by semiempirical PM3 computations that results in a cyclic hexamer where the amino terminal of one of the Glu interacts with the carboxylic end of the neighbor and so on, through hydrogen bonds (Figure 8a) (Supporting Information). In turn, the Glu-hexamer has been developed starting from dimer and then going through trimer, tetramer, and pentamer (Supporting Information) in a cascade fashion. The Glu-hexamer has a diameter of ~2.2 nm. The stabilization energy of the hexamer is commensurate with the H-bond interactions formed between them. The Glu-hexamer has its side-chain –COOH moiety projecting out and is suitable for further complexation with the amido-calix conjugate.

Thus the complexation of the side chain –COOH unit of each residue of the Glu-hexamer with one C4A-Phe-OH results in the hexameric aggregate shown in Figure 8b, and this has been computationally modeled by molecular mechanics. The structures of the Asp and Glu complexes of the amido conjugate as obtained from B3LYP/6-31G computations were taken in order to generate the hexameric clusters using the SymmDock web server.<sup>36,37</sup> Among the top ranked solutions generated, the best one was subjected to molecular mechanics calculations using the HYPERCHEM program.<sup>38</sup> The minimizations were done by using Polak–qRibiere conjugate gradient method by considering rms gradient of 0.1 kcal/mol. The resulting structures exhibit a bowl-shaped

arrangement with a rim diameter of ~3.2 and ~3.1 nm, and a bowl depth of ~1.6 and ~1.5 nm, respectively, for Glu and Asp complexes. The diameter of the channel observed in this structure is found to be  $0.55 \pm 0.05$  nm. Such structures are amenable for the formation of a dimer through the hydrophobic interaction between the rim portions of two bowls resulting in an almost spherical particle as shown in Figure 8c. About 50% of the surface area of such spherical particles is hydrophilic groups, while the rest is hydrophobic, and hence these can lead to the formation of higher size aggregates in 3 dimensions through hydrophobic and hydrophilic interactions to result in supramolecular structures already demonstrated through microscopy. These hexameric aggregates are reminiscent of the hexameric micellar structures shown for 1:1 complexes of  $\text{Ag}^+$  and calix[6]arene reported in the literature,<sup>39</sup> wherein the amino acid in the present case can be considered to be replaced by  $\text{Ag}^+$ , and the C4A-Phe-OH is being replaced by calix[6]arene.

**MALDI Studies.** The aggregational behavior of the Asp/Glu complex of C4A-Phe-OH has been further revealed based on MALDI mass spectrum (Supporting Information) which exhibited peaks at 5698.3 and 5696.5 respectively for Asp and Glu and are assignable to the oligomers, viz.,  $\{4 \times \text{C4A-Phe-OH} + 11 \times \text{Asp} + \text{H}\}^+$  (Figure 9) and  $\{4 \times \text{C4A-Phe-OH} + 10 \times \text{Glu} + 7\text{H}\}^+$ . No such oligomers were observed with the individual precursors, viz., C4A-Phe-OH or Asp or Glu.

**Formation of Nanospheres by GSH-AgNP with C4A-Phe-OH.** As the amido-calix conjugates were shown to recognize GSH through its side chain –COOH function and the Ag nanoparticles can be coated using –SH moiety of the GSH, the interaction between the GSH-coated Ag nanoparticles (GSH-AgNP), and these conjugates were studied by TEM and AFM. The GSH-AgNP have been characterized by absorption, TEM, and powder XRD techniques (Supporting Information), and the data was found to be comparable with that reported in the literature.<sup>40–42</sup>

(32) Zhurko, G. A.; Zhurko D. A. *ChemCraft*; <http://www.chemcraftprog.com>.

(33) Nemes, P.; Schlosser, G.; Vekey, K. *J. Mass spectrom.* **2005**, *40*, 43.

(34) Cooks, R. G.; Zhang, D.; Koch, K. J. *Anal. Chem.* **2001**, *73*, 3646.

(35) Nanita, S. C.; Cooks, R. G. *Angew. Chem., Int. Ed.* **2006**, *45*, 554.

(36) Duhovery, D.; Nussinov, R.; Wolfson, H. J. In *Algorithms in Bioinformatics: Second International Workshop*; Guigo, R., Gusfield, D., Eds.; WABI 2002, Rome, Italy, Lecture Notes in Computer Science 2452; Springer Verlag: New York, 2002; p 185.

(37) Zhang, C.; Vasmatzis, G.; Cornette, J. L.; DeLisi, C. *J. Mol. Biol.* **1997**, *267*, 707.

(38) HyperChem 8.0.4; Hypercube, Inc.: Gainesville, FL, 2007.

(39) Houmadi, S.; Coquière, D.; Legrand, L.; Faur, M. C.; Goldmann, M.; Reinaud, O.; Rmita, S. *Langmuir* **2007**, *23*, 4849.

(40) Jiang, X.; Xie, Y.; Lu, J.; Zhu, L.; He, W.; Qian, Y. *Langmuir* **2001**, *17*, 3795.

**TEM Studies.** In TEM, the GSH-AgNP (see Experimental Section) were mainly found to be of  $\sim 7$  nm in size, as can be seen from Figure 10a (Supporting Information). When C4A-Phe-OH was added to GSH-AgNP, the nanospecies were further aggregated into spherical clusters resulting in nanospheres with diameters ranging from 60 to 120 nm (Figure 10b–d). Similar studies carried out with an amido

conjugate-ester, namely, C4A-Phe-OMe, resulted in no nanospheres, suggesting that the terminal arm  $-COOH$  moiety is necessary for the formation of nanospheres. Further studies carried out with amido-calix conjugates that do not possess a phenyl side chain, viz., C4A-Gly-OH and C4A-Ala-OH, also resulted in no nanospheres, suggesting the necessity of the phenyl moiety in forming these (Figure 10e–g). The TEM results clearly support the role of hydrophobic interactions in the formation of nanospheres. Thus, it may be visualized that the nanospheres observed in TEM result from the complexation of GSH-AgNP with C4A-Phe-OH as 1:1 complexes followed by the hydrophobic interactions extended between the side chain phenyl moieties of the neighbor silver nanoparticles.

**AFM Studies.** Experiments similar to that reported under TEM were performed even by AFM, and the formation of nanospheres was found only in the case of C4A-Phe-OH (Figure 11) and not with C4A-Phe-OMe or C4A-Gly-OH or C4A-Ala-OH (Figure 12), suggesting the importance of the terminal  $-COOH$  and the side chain phenyl moiety present on the calix arms in the formation of these spheres. The size of GSH-AgNP was found to be in the range of 23–36 nm

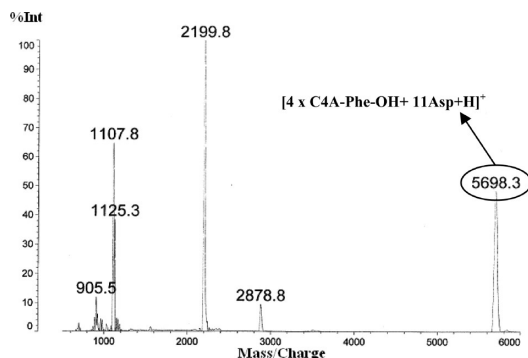


FIGURE 9. MALDI-TOF spectra for [C4A-Phe-OH + Asp].

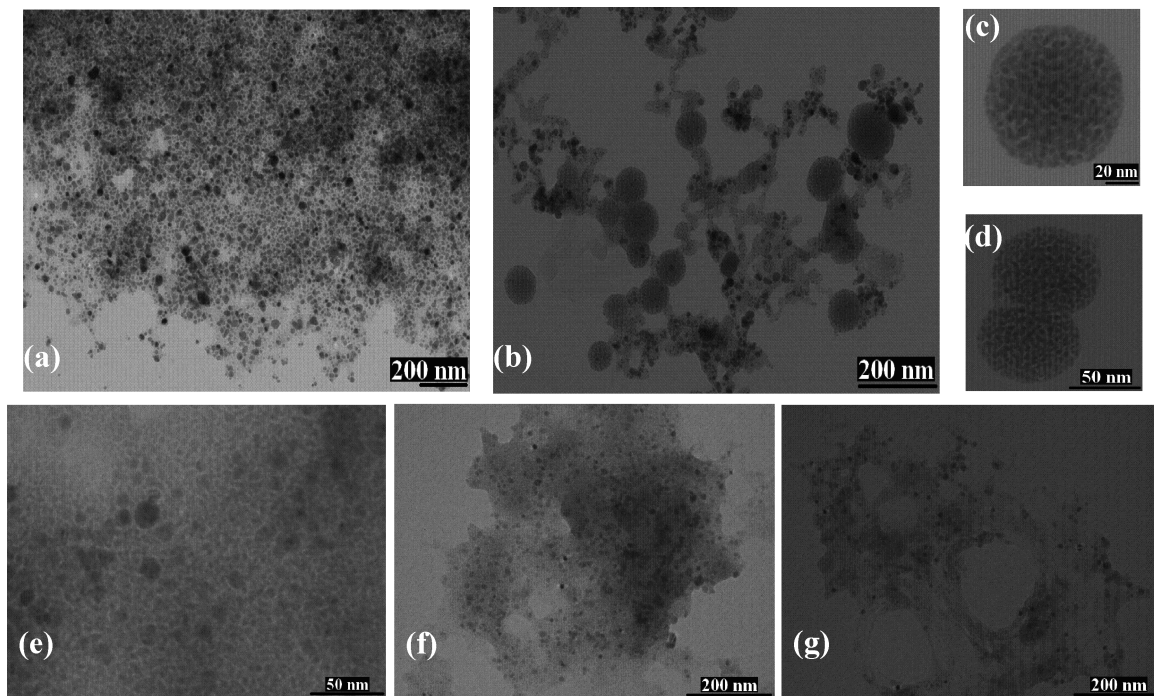


FIGURE 10. Transmission electron micrographs of (a) GSH-capped silver nanoparticles (GSH-AgNP), (b) nanospheres formed by {GSH-AgNP + C4A-Phe-OH} [(c, d) are the magnified version of two different nanospheres seen in (b)], (e) {GSH-AgNP + C4A-Phe-OMe}, (f) {GSH-AgNP + C4A-Gly-OH}, and (g) {GSH-AgNP + C4A-Ala-OH}.

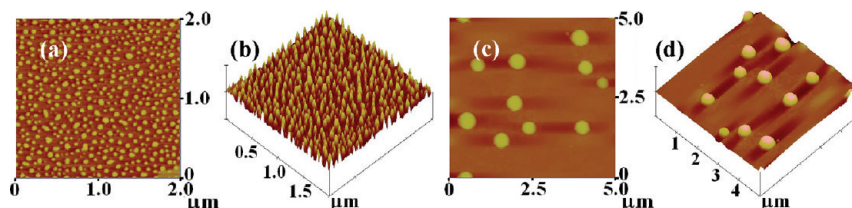


FIGURE 11. Atomic force microscopy images of (a) GSH-capped silver nanoparticles (GSH-AgNP), (b) 3D view of that given in (a), (c) nanospheres formed by {(GSH-AgNP) + C4A-Phe-OH}, and (d) 3D view of that given in (c).

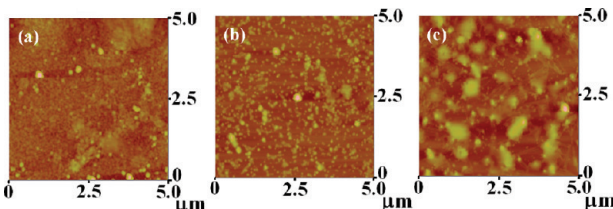
when deposited on a mica surface. When C4A-Phe-OH was added to GSH-AgNP, nanospheres of sizes  $\sim$ 480–520 nm were observed. Thus the nanospheres formed were about 10–20 times bigger than the simple GSH-AgNP in both TEM as well as in AFM.

**Studies Extended to Proteins.** Albumins are most abundantly found and well studied circulatory proteins possessing greater  $\alpha$ -helical content. Bovine serum albumin (BSA), human serum albumin (HSA), and  $\alpha$ -lactalbumin possess  $\sim$ 14–16% Asp and Glu residues. Since several of these amino

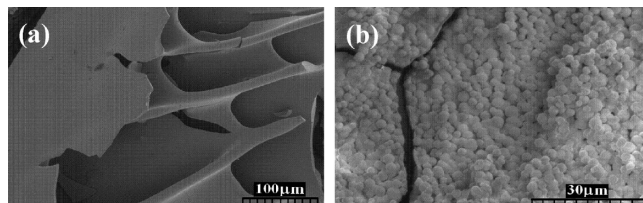
acids are present on the surface of the protein, the side chain –COOH groups can complex with amido-calix conjugates through the interactions analogous to that observed between the amido conjugate and Asp/Glu. However, in the case of proteins, such interactions may further lead to specific changes in their aggregational behavior, and the resulting structures may be distinguishable from the nanostructures of the simple protein. Thus it is of interest to monitor the changes observed in microscopy features of the proteins and their complexes.

**SEM Studies.** To support the interactions present between C4A-Phe-OH and BSA/HSA, SEM studies have been carried out. SEM of the corresponding complex of {HSA + C4A-Phe-OH} exhibited almost uniformly spherical particles (Figure 13a,b). The sizes of these protein-bound particles are larger by at least about 10 times compared to those observed with simple aspartic acid complex (Figure 6b,c).

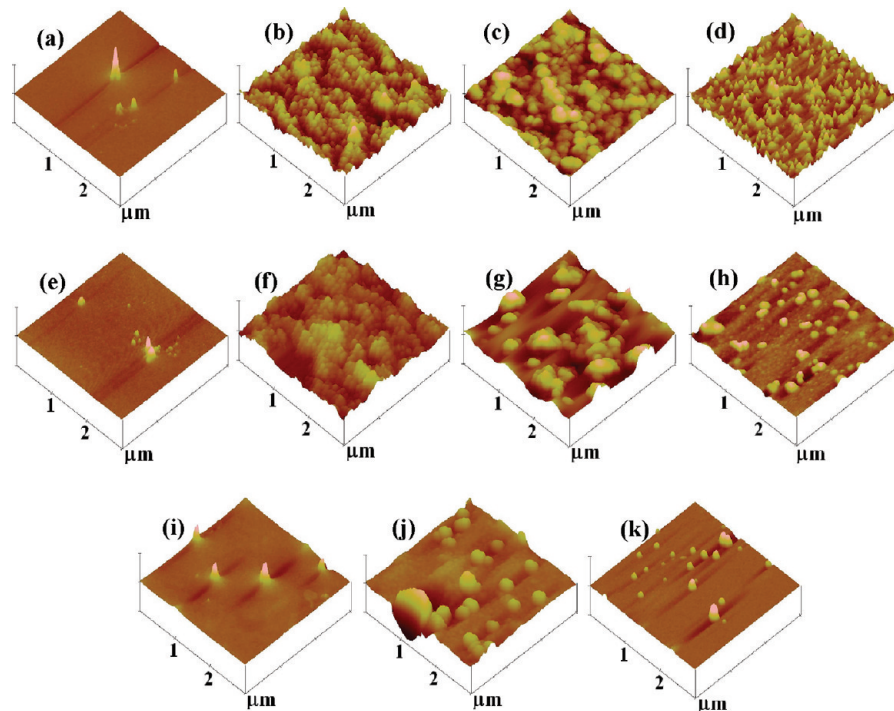
**AFM Studies.** When C4A-Phe-OH was added to BSA/HSA, the proteins tend to agglomerate (Figure 14b,f) and result in particles with distorted spherical shape, as can be seen from the micrographs. Though the size of these particles does not seem to change much ( $\sim$ 90–150 nm in free protein compared to  $\sim$ 100–180 nm in complexed species), the height of the particles has been found to change considerably ( $\sim$ 4–20 nm in free protein compared to 18–60 nm in complexed species). On the other hand, the aggregation that results from the interaction of C4A-Gly-OH and BSA/HSA results in almost spherical particles (Figure 14c,g). This suggests that the nanospheres formed between the amido-calix conjugates and BSA/HSA seem to be dependent only on the presence of the amido arm and not the side chain. This may be attributable to the arene basket present in these conjugates. Similar studies carried out with the –COOMe terminal, namely, C4A-Phe-OMe, resulted in much less



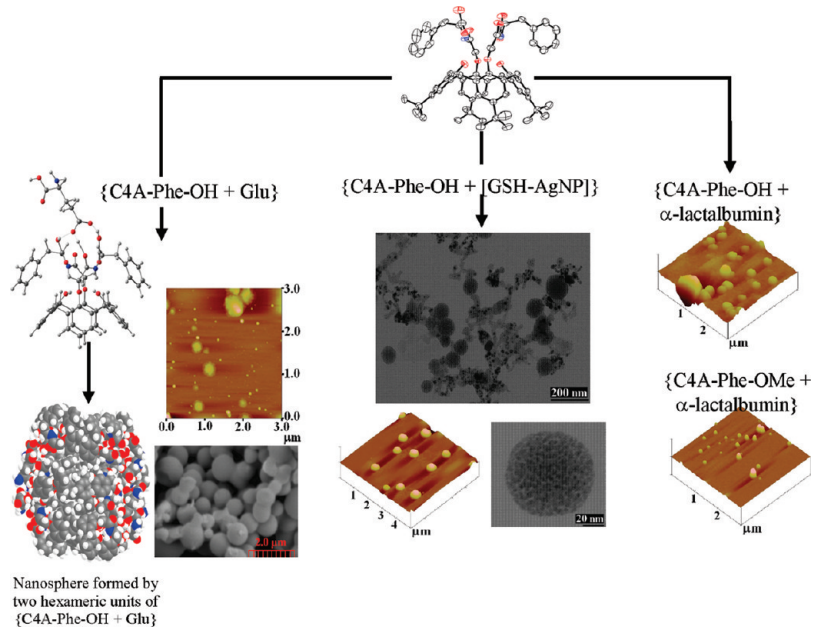
**FIGURE 12.** Atomic force microscopy images of (a) {(GSH-AgNP) + C4A-Gly-OH}, (b) {(GSH-AgNP) + C4A-Ala-OH}, and (c) {(GSH-AgNP) + C4A-Phe-OMe}.



**FIGURE 13.** Scanning electron micrographs of (a) HSA and (b) {C4A-Phe-OH + HSA}.



**FIGURE 14.** Atomic force microscopy images of (a) BSA, (b) {C4A-Phe-OH + BSA}, (c) {C4A-Gly-OH + BSA}, (d) {C4A-Phe-OMe + BSA}, (e) HSA, (f) {C4A-Phe-OH + HSA}, (g) {C4A-Gly-OH + HSA}, (h) {C4A-Phe-OMe + HSA}, (i)  $\alpha$ -lactalbumin, (j) {C4A-Phe-OH +  $\alpha$ -lactalbumin}, and (k) {C4A-Phe-OMe +  $\alpha$ -lactalbumin}.

**SCHEME 2. Microscopy Features of the Recognition of Glu, GSH-AgNP, and  $\alpha$ -Lactalbumin by C4A-Phe-OH**


aggregation than that observed in the case of C4A-Phe-OH (Figure 14d,h), suggesting the positive role played by the terminal  $-COOH$  of the arms of the conjugates. Similar results were observed even with the  $\alpha$ -lactalbumin, which is also an  $\alpha$ -helical protein (Figure 14j,k)

### Conclusions and Correlations

To our knowledge, this is the first report wherein an amido-calix[4]arene conjugate and its amino acid/peptide/protein complexes have been differentiated on the basis of spectroscopy and microscopy studies followed by modeling of the species by computational studies. In the present paper, several amido-calix[4]arene conjugates were synthesized and characterized, and structures of a few of these were established by single crystal XRD. All these were studied for their selective recognition toward amino acids Asp and Glu and the peptides GSH and GSSG and were compared with some appropriate control molecular systems. The fluorescence data obtained in the present case certainly exhibit higher association constants (i.e.,  $532/676\text{ M}^{-1}$ ) as compared to that reported in the literature ( $16-63\text{ M}^{-1}$ <sup>10</sup>) by exhibiting a *switch on* fluorescence. It has been shown as 1:1 complex by mass spectrometry. The studies clearly supported the need for the calix[4]arene platform, amido arm, and terminal  $-COOH$  moiety in the recognition toward amino acids and peptides possessing side chain  $-COOH$  moiety. The structural features of the 1:1 complex formed between amido-calix conjugate and Asp/Glu/GSH have been derived on the basis of DFT computational calculations, wherein the complex is stabilized through three intermolecular hydrogen bond interactions.

Thus, amido-calix conjugates reported in this paper are potential receptors that can bind to Asp/Glu residues by sensing their side chain  $-COOH$  moiety as well as those

present in the tripeptide, viz., GSH/GSSG. Studies based on AFM and SEM resulted in the formation of spherical particles followed by reduction in the particle size by about 100-fold upon complexation when compared to the particles of uncomplexed conjugate, namely, C4A-Phe-OH. These results were supported by DLS studies. The spherical particle has been modeled by semiempirical (PM3) followed by molecular mechanics (MM+) computations as hexameric aggregates that are reminiscent of the hexameric micellar structures shown for 1:1 complexes of  $Ag^+$  and calix[6]arene reported in the literature.<sup>39</sup> The aggregation of such nanoscopic species through interspecies interactions can lead to the formation of the type of particles observed in the microscopy studies. This has been further supported by studying the microscopy of the structures formed by the complexes of the amido-calix conjugates with GSH-AgNP. The TEM and AFM studies clearly demonstrate the necessity and the role of terminal  $-COOH$  moiety of the arm and the side chain of the amido unit in the formation of the nanospheres.

Since the recognition and the formation of the nanospheres is through the side chain  $-COOH$  function, the studies were extended to  $\alpha$ -helical proteins, viz., BSA, HSA, and  $\alpha$ -lactalbumin, and it was found that the principle observed in the amino acid studies can indeed be applied to these proteins. The aggregational behavior of these proteins as studied by AFM clearly differentiates the nanostructural features of the simple proteins from their complexes. The present paper clearly provided the nanostructural differences in the recognition of amido-calix conjugates toward Asp/Glu and albumin proteins as can be seen from the Scheme 2 given in the case of C4A-Phe-OH and C4A-Phe-OMe.

Thus the present study throws light on the manner in which protein aggregations are induced in the biological systems. Hence the results reported in this paper may find implications in medical diagnosis and drug delivery when the studies are extended appropriately, which can indeed be monitored through spectroscopy and microscopy methods.

(41) Slocik, J. M.; Wright, D. W. *Biomacromolecules* **2003**, *4*, 1135.  
(42) Lieberman, I.; Shemer, G.; Fried, T.; Kosower, E. M.; Markovich, G. *Angew. Chem., Int. Ed.* **2008**, *47*, 4855.

## Experimental Section

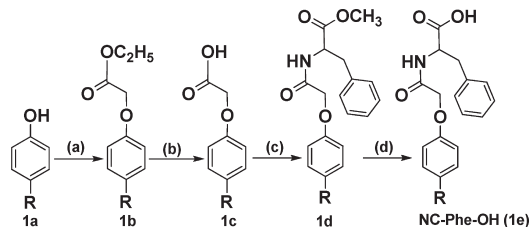
**Synthesis and Characterization Data.** The *p*-*tert*-butyl-calix[4]arene (**C4A**) has been synthesized by the condensation of *p*-*tert*-butyl-phenol with formaldehyde in presence of NaOH as per the procedure given by Gutsche and co-workers.<sup>26</sup> Synthesis for **C4A-OEt**, **C4A-OH** and **C4A-Phe-OMe** have already been reported by us earlier,<sup>27</sup> and hence only the characterization data for these is given in this section.

**C4A-Phe-OMe.**  $C_{68}H_{82}N_2O_{10}$  (1086): Anal. (% found) C 74.75, H 7.20, N 2.75; (% required) C 75.14, H 7.55, N 2.58. FTIR (KBr,  $\text{cm}^{-1}$ ): 3458, 3304 ( $\nu_{\text{NH}/\text{OH}}$ ), 1752 ( $\nu_{\text{C=O}}, \text{COOMe}$ ), 1670 ( $\nu_{\text{C=O}}, \text{CONH}$ ).  $^1\text{H}$  NMR ( $\text{CDCl}_3$ ,  $\delta$  ppm): 1.02, 1.30 (s, 36H,  $\text{C}(\text{CH}_3)_3$ ), 3.02–3.15 (m, 6H, Ar- $\text{CH}_2$ -Ar, and  $\text{C}^\beta\text{H}_2$ -Ph), 3.47 (d, 2H, Ar- $\text{CH}_2$ -Ar,  $J = 13.76$  Hz), 3.64 (s, 6H,  $\text{OCH}_3$ ), 4.06 (d, 2H, Ar- $\text{CH}_2$ -Ar,  $J = 12.9$  Hz), 4.10 (d, 2H, Ar- $\text{CH}_2$ -Ar,  $J = 14.2$  Hz), 4.14 (d, 2H, O- $\text{CH}_2$ -CO,  $J = 15.2$  Hz), 5.03 (d, 2H, O- $\text{CH}_2$ -CO,  $J = 15.0$  Hz), 5.10 (q, 2H,  $\text{C}^\alpha\text{H}$ ,  $J = 7.8, 7.0$  Hz), 6.87 (d, 4H, Ar- $H$ ), 7.03 (m, 14H, Ar- $H$ , Ph- $H$ ), 7.73 (s, 2H, OH), 9.51 (d, 2H, NH,  $J = 8.3$ ).  $^{13}\text{C}$  NMR ( $\text{CDCl}_3$ ):  $\delta$  30.9, 31.7 ( $\text{C}(\text{CH}_3)_3$ ), 32.0, 32.5 (Ar- $\text{CH}_2$ -Ar), 33.9, 34.0 (*tert*-C), 39.0 ( $\text{CH}_2$ -Ph), 52.1 ( $\text{OCH}_3$ ), 52.8 (CH), 74.9 (O- $\text{CH}_2$ -CO), 124.7, 125.3, 125.8, 126.4, 126.5, 126.7, 127.6, 128.1, 128.9, 132.6, 136.1, 142.3, 147.8, 149.7, 150.0 (aromatic carbons), 168.8 (CONH), 171.8 (COOMe) ppm. ES-MS:  $m/z = 1087$  ([M + H]<sup>+</sup>, 100%).

**C4A-Phe-OH.** To THF (15 mL) was added **C4A-Phe-OMe** (1.086 g, 1 mmol), and the mixture was stirred at 0 °C. LiOH (0.126 g, 3 mmol) in water (2 mL) was added to this at 0 °C, and the mixture was brought to room temperature and was stirred for 6 h. The solvent was removed under reduced pressure to give a gel-like yellow substance. To this was added chilled water, and the mixture was acidified with 1 N HCl (pH ~1) to give a white solid. The product was filtered, washed with water, and then dried to yield a white solid. Yield: 0.952 g (90%); mp 180–182 °C. FTIR (KBr): 3424 ( $\nu_{\text{OH}}$ ), 3336, 1741 ( $\nu_{\text{C=O}}, \text{COOH}$ ), 1654 ( $\nu_{\text{C=O}}, \text{CONH}$ )  $\text{cm}^{-1}$ .  $^1\text{H}$  NMR (DMSO- $d_6$ ):  $\delta$  1.10 (s, 18H,  $\text{C}(\text{CH}_3)_3$ ), 1.21 (s, 18H,  $\text{C}(\text{CH}_3)_3$ ), 3.09–3.16 (m, 4H,  $\text{CH}_2$ -Ph), 3.33 (d, 2H, Ar- $\text{CH}_2$ -Ar,  $J = 12.9$  Hz), 3.38 (d, 2H, Ar- $\text{CH}_2$ -Ar,  $J = 12.9$ ), 4.16 (d, 2H, Ar- $\text{CH}_2$ -Ar  $J = 12.8$  Hz), 4.25 (d, 2H, Ar- $\text{CH}_2$ -Ar  $J = 12.9$  Hz), 4.48 (m, 4H,  $\text{OCH}_2\text{CO}$ ), 4.64 (q, 2H,  $\text{C}^\alpha\text{H}$ ,  $J = 6.22$  Hz), 7.08 (s, 4H, Ar- $H$ ), 7.12–7.21 (m, 14H Ar- $H$  + phe- $H$ ), 8.16 (s, 2H, OH), 8.72 (d, 2H, NH,  $J = 7.63$  Hz) ppm.  $^{13}\text{C}$  NMR (DMSO- $d_6$ ):  $\delta$  30.8, 31.4 ( $\text{C}(\text{CH}_3)_3$ ), 33.6, 33.9 (*tert*-C), 36.8 ( $\text{C}^\beta\text{H}_2\text{Ph}$ ), 53.6 ( $\text{C}^\alpha\text{H}$ ), 74.1 ( $\text{OCH}_2\text{CO}$ ), 125.4, 125.8, 126.3, 127.0, 127.2, 128.1, 129.1, 132.7, 132.8, 137.3, 141.5, 147.2, 149.8, 150.5, (aromatic carbon resonances), 168.0 (C=O CONH), 172.4 (C=O COOH) ppm. ES-MS:  $m/z = 1059$  ([M + H]<sup>+</sup>, 100%). Anal. Calcd for  $\text{C}_{66}\text{H}_{78}\text{N}_2\text{O}_{10}\cdot\text{H}_2\text{O}$  (1076): C, 73.58; H, 7.48; N, 2.60. Found: C, 73.37; H, 7.29; N, 2.70 (Supporting Information).

**C4A-Gly-OH.** Yield 0.781 g (89%); mp 210 °C (decomposes). FTIR (KBr): 3440 ( $\nu_{\text{OH}}$ ), 1747 ( $\nu_{\text{C=O}}, \text{COOH}$ ); 1662 ( $\nu_{\text{C=O}}, \text{CONH}$ )  $\text{cm}^{-1}$ .  $^1\text{H}$  NMR (DMSO- $d_6$ ):  $\delta$  1.13 (s, 18H,  $\text{C}(\text{CH}_3)_3$ ), 1.20 (s, 18H,  $\text{C}(\text{CH}_3)_3$ ), 3.47 (d, 4H, Ar- $\text{CH}_2$ -Ar,  $J = 13.2$  Hz), 4.03 (m, 4H,  $\text{C}^\alpha\text{H}_2$ ), 4.23 (d, 4H, Ar- $\text{CH}_2$ -Ar,  $J = 12.8$  Hz), 4.53 (s, 4H,  $\text{OCH}_2\text{CO}$ ), 7.17 (s, 8H, Ar- $H$ ), 8.41 (s, 2H, OH), 8.89 (t, 2H, HN) ppm.  $^{13}\text{C}$  NMR (DMSO- $d_6$ ):  $\delta$  31.1, 31.6 ( $\text{C}(\text{CH}_3)_3$ ), 33.8, 34.2 ( $\text{C}(\text{CH}_3)_3$ ), 40.6 ( $\text{C}^\alpha\text{H}_2$ ), 72.1 (*tert* C), 74.3 ( $\text{OCH}_2\text{CO}$ ), 125.5, 125.9, 127.1, 133.0, 141.6, 147.5, 149.8, 150.1 (aromatic carbons), 168.7 (C=O CONH), 170.8 (C=O, COOH) ppm. ESI-MS:  $m/z = 901$  ([M + Na]<sup>+</sup>, 100%). Anal. Calcd for  $\text{C}_{52}\text{H}_{66}\text{N}_2\text{O}_{10}\cdot 3\text{H}_2\text{O}$  (932): C, 66.93; H, 7.78; N, 3.00. Found: C, 66.71; H, 7.72; N, 2.86.

**C4A-Ala-OH.** Yield 0.843 g (93%); mp 196–198 °C. FTIR (KBr): 3443, 3329, 1745 ( $\nu_{\text{C=O}}, \text{COOH}$ ); 1661 ( $\nu_{\text{C=O}}, \text{CONH}$ )  $\text{cm}^{-1}$ .  $^1\text{H}$  NMR (DMSO- $d_6$ ):  $\delta$  1.12 (s, 18H,  $\text{C}(\text{CH}_3)_3$ ), 1.20 (s, 18H,  $\text{C}(\text{CH}_3)_3$ ), 1.40 (d, 6H,  $\text{CH}_3$ -ala,  $J = 7.27$  Hz), 3.45

SCHEME 3. Synthesis of NC-Phe-OH<sup>a</sup>

<sup>a</sup>(a) Acetone,  $\text{K}_2\text{CO}_3$ ,  $\text{BrCH}_2\text{COOEt}$ , reflux for 15 h; (b) EtOH, aq NaOH, reflux for 24 h; (c) Phe-OMe.HCl, dry THF,  $\text{Et}_3\text{N}$ , HOBT, DCC; (d) THF, LiOH. R = *tert*-butyl.

(d, 2H, Ar- $\text{CH}_2$ -Ar,  $J = 12.9$  Hz), 3.54 (d, 2H, Ar- $\text{CH}_2$ -Ar,  $J = 13.1$  Hz), 4.15 (d, 2H, Ar- $\text{CH}_2$ -Ar,  $J = 13.1$  Hz), 4.31 (d, 2H,  $\text{OCH}_2\text{CO}$ ,  $J = 15.1$  Hz), 4.41–4.36 (m, 2H each, Ar- $\text{CH}_2$ -Ar +  $\text{C}^\alpha\text{H}$ ), 4.77 (d, 2H,  $\text{OCH}_2\text{CO}$ ,  $J = 15.1$  Hz), 7.22–7.17 (m, 8H, Ar- $H$ ), 8.30 (s, 2H, OH), 9.09 (d, 2H, HN,  $J = 7.6$  Hz) ppm.  $^{13}\text{C}$  NMR (DMSO- $d_6$ ):  $\delta$  17.0 ( $\text{C}^\beta\text{H}_3$ ), 30.8, 31.1 ( $\text{C}(\text{CH}_3)_3$ ), 30.9 (Ar- $\text{CH}_2$ -Ar), 31.9 (Ar- $\text{CH}_2$ -Ar), 33.6, 34.0 ( $\text{C}(\text{CH}_3)_3$ ), 47.8 ( $\text{C}^\alpha\text{H}$ ), 74.5 ( $\text{OCH}_2\text{CO}$ ), 125.1, 125.6, 125.8, 126.4, 126.7, 127.4, 132.6, 132.9, 142.0, 147.7, 149.3, 150.0 (aromatic carbons), 167.7 (C=O CONH), 173.7 (C=O COOH) ppm. FABMS:  $m/z = 913$  ([M + Li]<sup>+</sup>, 100%). Anal. Calcd for  $\text{C}_{54}\text{H}_{70}\text{N}_2\text{O}_{10}\cdot 4\text{H}_2\text{O}$  (978): C, 66.23; H, 8.03; N, 2.86. Found: C, 66.40; H, 7.73; N, 2.67.

**NC-Phe-OH (1e).** Control molecule **1e** has been synthesized as shown in Scheme 3, and the characterization data has been given under Supporting Information. Compounds **1b** and **1c** have already been reported by us.<sup>27</sup>

**1d.** To a solution of **1c** (0.5 g, 2.40 mmol) in  $\text{CH}_2\text{Cl}_2$  (70 mL) were added  $\text{Et}_3\text{N}$  (1.7 mL, 12 mmol), 1-ethyl-(3-dimethylaminopropyl)-3-carbodiimide hydrochloride (EDCI·HCl) (0.70 g, 3.6 mmol), and a catalytic amount of 1-hydroxybenzotriazole (HOBT), and the mixture was stirred at 0 °C for 30 min under  $\text{N}_2$  atmosphere. L-Phenylalaninemethylester hydrochloride (0.73 g, 3.36 mmol) was added to this reaction mixture and stirred at room temperature for overnight. The resulting mixture was washed with water followed by saturated  $\text{NaHCO}_3$  and brine. The organic residue was dried using sodium sulfate. Organic solvent was removed under reduced pressure to result in a highly viscous light yellowish oily liquid. This product was used for the next step without further purification. Yield (0.55 g, 65%).  $\text{C}_{22}\text{H}_{27}\text{NO}_4$  (369.45).  $^1\text{H}$  NMR ( $\text{CDCl}_3$ ,  $\delta$  ppm): 1.24 (s, 9H,  $\text{C}(\text{CH}_3)_3$ ), 3.06 (t, 2H,  $J = 6$  Hz, Ph- $\text{CH}_2$ ), 3.65 (s, 3H,  $\text{OCH}_3$ ), 4.4 (s, 2H,  $\text{OCH}_2$ ), 4.89 (q, 1H,  $J = 14$  Hz, CH), 6.72 (d, 2H,  $J = 10$  Hz, Ar- $H$ ), 6.97 (m, 1H,  $J = 10$  Hz, Ar- $H$ ), 7.13 (d, 2H,  $J = 2$  Hz, Ar- $H$ ), 7.16 (d, 2H,  $J = 2$  Hz, Ar- $H$ ), 7.23 (m, 2H, Ar- $H$ ).  $^{13}\text{C}$  NMR: ( $\text{CDCl}_3$ ,  $\delta$  ppm): 31.6, 38.1, 41.2, 52.5, 52.7, 67.5, 114.4, 126.6, 126.9, 127.3, 128.7, 129.3, 135.6, 145.1, 155.1, 168.3, 171.6. ESI-MS:  $m/z$  (intensity (%), fragment) 370.04. (100, [M + H]<sup>+</sup>).

**1e.** To THF (50 mL) was added **1d** (1.086 g, 1 mmol), and the mixture was stirred at 0 °C. LiOH (0.126 g, 3 mmol) in water (2 mL) was added to this at 0 °C, and the mixture was brought to the room temperature and was stirred for 6 h. The solvent was removed under reduced pressure to give a gel-like yellow substance. To this, chilled water was added and acidified with 1 N HCl (pH ~1). The compound was separated by organic layer. It was dried using sodium sulfate and concentrated under reduced pressure to give a yellowish liquid. To this was added diethyl ether, and the mixture was kept overnight. A white solid was formed next day. Yield: (0.42 g, 75%);  $\text{C}_{21}\text{H}_{25}\text{NO}_4$  (355.42).  $^1\text{H}$  NMR ( $\text{CDCl}_3$ ,  $\delta$  ppm): 1.22 (s, 9H,  $\text{C}(\text{CH}_3)_3$ ), 3.10 (t, 2H,  $J = 13$  Hz, Ph- $\text{CH}_2$ ), 4.4 (s, 2H,  $\text{OCH}_2$ ), 4.90 (q, 1H,  $J = 8$  Hz, CH), 6.70 (d, 2H,  $J = 9$  Hz, Ar- $H$ ), 7.01 (m, 1H,  $J = 9$  Hz, Ar- $H$ ), 7.15

(d, 2H,  $J = 2$  Hz, Ar-H), 7.17 (d, 2H,  $J = 2$  Hz, Ar-H), 7.23 (m, 2H, Ar-H).  $^{13}\text{C}$  NMR ( $\text{CDCl}_3$ ,  $\delta$  ppm): 31.6, 34.3, 37.5, 52.6, 67.4, 114.4, 126.6, 127.4, 128.8, 129.4, 135.4, 145.1, 155.0, 169.2, 174.5. ESI-MS:  $m/z$  (intensity (%), fragment) 356.03. (100,  $[\text{M} + \text{H}]^+$ ) (Supporting Information).

**Fluorescence Studies.** Fluorescence emission spectra were measured by exciting the solutions of C4A-Phe-OH/C4A-Gly-OH/C4A-Ala-OH and the control molecules at 280 nm, and the emission spectra were recorded in the 290–450 nm range. The bulk solutions of C4A-Phe-OH/C4A-Gly-OH/C4A-Ala-OH and other control molecules were prepared in  $\text{CH}_3\text{OH}$  except in the case of the aqueous  $\text{CH}_3\text{CN}$  solvent system in which  $\text{CH}_3\text{CN}$  was used for bulk solution preparation. All the measurements were made in 3 cm quartz cells, and a final ligand concentration of 5  $\mu\text{M}$  was maintained. During the titration, the concentration of amino acids/peptides was varied accordingly in order to result in requisite mole ratios of amino acids/peptides, and the total volume of the solution was maintained constant at 3 mL in each case by adding appropriate solvent or solvent mixtures. Normalized emission (relative fluorescence) intensities ( $I/I_0$ ) (where  $I_0$  is the intensity with no amino acid addition;  $I$  is the intensity at different mole ratios of amino acid to ligand) were plotted against the mole ratio of amino acid to ligand. The association constant of the amino acid formed in the solution has been estimated using the standard Benesi–Hildebrand equation, viz.,

$$\frac{1}{I - I_0} = \frac{1}{I_1 - I_0} + \frac{1}{(I_1 - I_0)K_a[\text{AA}]}$$

where  $I_0$  is the intensity of ligand,  $I$  is the intensity in the presence of amino acid,  $I_1$  is intensity upon saturation with amino acid,  $[\text{AA}]$  is the concentration of amino acid, and  $K_a$  is the association constant of the complex formed.

**Computational Optimization of the Complex Formed.** The starting geometry of C4A-Phe-OH has been taken from the crystallographic coordinates.<sup>28</sup> In view of the large computational times involved, C4A-Phe-OH has been truncated to give precursor C4A-Phe-OH' by replacing each *tert*-butyl group present at the upper rim of the calix[4]arene with a hydrogen without affecting the conformation of the calix[4]arene ring. The geometry optimizations of the precursors (viz., C4A-Phe-OH' and Asp/Glu/GSH) and the complex have been carried out in a cascade fashion by starting from a semiempirical method and ending with DFT as shown in this sequence, viz., AM1 → HF/3-21G → HF/6-31G → B3LYP/3-21G → B3LYP/6-31G. The initial structures for the complexes were modeled by taking the DFT optimized structure of C4A-Phe-OH' and Asp or Glu or GSH, wherein the precursors were placed at a noninteracting distance and further optimized in the cascade fashion. Similar computations were carried out even with the *tert*-butyl truncated version of C4A-Gly-OH (C4A-Gly-OH').

**AFM Studies.** Tapping mode with a phosphorus-doped Si probe having sharp fine tip at the end was used for all of the studies. The sample of C4A-Phe-OH/C4A-Gly-OH/C4A-Ala-OH for AFM was prepared from a  $3 \times 10^{-4}$  M solution in methanol. The solution for the aspartic acid/glutamic acid complex of C4A-Phe-OH were prepared by mixing 50  $\mu\text{L}$  of C4A-Phe-OH and 200  $\mu\text{L}$  of aspartic acid/glutamic acid ( $3 \times 10^{-3}$  M) in methanol. All samples for AFM studies were

prepared by sonicating the corresponding solutions for approximately 30 min. About 5–10  $\mu\text{L}$  of the sonicated solutions was spread on mica sheets as substrate and were allowed to air-dry. The dried substrates were taken for AFM measurements.

For AFM studies with GSH-AgNP, 50  $\mu\text{L}$  of GSH-AgNP was added to 50  $\mu\text{L}$  of  $3 \times 10^{-4}$  M solution of C4A-Phe-OH/C4A-Gly-OH/C4A-Ala-OH/C4A-Phe-OME.

For AFM studies with proteins, 100  $\mu\text{L}$  of protein (1 mg/10 mL) was added to 100  $\mu\text{L}$  of C4A-Phe-OH/C4A-Gly-OH/C4A-Ala-OH/C4A-Phe-OME.

**Dynamic Light Scattering Studies.** The hydrodynamic diameter of all the samples were measured in methanol (concentration were kept same as in the case of fluorescence studies) at 25 °C. The incident laser (Coherent Inc. Santa Clara, CA) radiation used was 633 nm, wavelength of 90°. The scattered light was filtered through a vertical polarization filter. The experiments were carried out using standard cylindrical BI-RC 12 glass cuvettes. The concentrations of the samples were kept same as in fluorescence studies and the solvo-dynamic diameters have been measured for 1:4 mol ratio of Asp/Glu and C4A-Phe-OH.

**SEM Studies.** The powder samples were isolated from C4A-Phe-OH, Asp, Glu, and mixtures of {C4A-Phe-OH + Asp} or {C4A-Phe-OH + Glu} or corresponding protein samples. The surface of these powder samples were coated with gold and used for SEM.

**Preparation of GSH-AgNP.** Ag(0) nanoparticles have been prepared by a reported procedure with required modifications.<sup>40–42</sup> Sixty-eight milliliters of  $\text{AgNO}_3$  ( $2.5 \times 10^{-2}$  M) was taken in a flask and stirred vigorously for 5 min. Fifty milliliters of GSH ( $0.3 \times 10^{-2}$  M) was slowly added from a dropping funnel at a constant rate. The solution was stirred for another 30 min. To this solution was added 16 mL of  $\text{NaBH}_4$  ( $10^{-1}$  M). The solution immediately changes its color from yellow to brown. Vigorous stirring was continued for 8 h in dark. Precipitation of the product was done by adding absolute ethanol. The product was isolated by repeated centrifugation at 10,000 rpm.

**TEM Sample Preparation.** Approximately 5–10  $\mu\text{L}$  of an aqueous solution of GSH-AgNP (after sonication) was used for TEM studies. For studies with GSH-AgNP, the concentration of C4A-Phe-OH/C4A-Gly-OH/C4A-Ala-OH/C4A-Phe-OME was kept  $3 \times 10^{-4}$  M. Fifty microliters of C4A-Phe-OH/C4A-Gly-OH/C4A-Ala-OH/C4A-Phe-OME was mixed with 50  $\mu\text{L}$  of GSH-AgNP and sonicated for 30 min. Approximately 5–10  $\mu\text{L}$  of this solution was placed in the carbon-coated copper grid and allowed to air-dry.

**Acknowledgment.** C.P.R. acknowledges financial support from DST, CSIR, and DAE-BRNS. A.A. and J.P.C. acknowledge CSIR for SRF. We thank IIT Bombay for AFM (DST-FIST, Department of Physics), SEM (at MEMS), and DLS and TEM (at SAIF) facilities.

**Supporting Information Available:** Characterization data, crystallographic data, fluorescence data, ESI MS data, computational data, AFM and SEM data, MALDI TOF data, and UV-vis, powder XRD, and TEM data for GSH-AgNP. This material is available free of charge via the Internet at <http://pubs.acs.org>.